M-3029

J. Chem. Thermodynamics **1994,** 26, 987–1000

Phase stability and structural properties of $Ni_{7\pm\delta}S_6$ and Ni_9S_8 Heat capacity and thermodynamic properties of Ni_7S_6 at temperatures from 5 K to 970 K and of Ni_9S_8 from 5 K to 673 K

Svein Stølen, Helmer Fjellvåg, Fredrik Grønvold, Helene Seim,

Department of Chemistry, University of Oslo, P.O. Box 1033, Blindern, N-0315 Oslo, Norway

and Edgar F. Westrum, Jr.

Department of Chemistry, University of Michigan, Ann Arbor, MI 48109, U.S.A.

(Received 24 March 1994)

Two stable solid phases with composition in the range from (45 to 48) moles per cent of S exist for (nickel + sulfur): Ni_9S_8 which disproportionates to $Ni_{1-\delta}S$ and $Ni_{7\pm\delta}S_6$ above $T = (709 \pm 5)$ K, and $Ni_{7\pm\delta}S_6$. The latter non-stoichiometric phase forms eutectoidally from Ni_9S_8 and Ni_3S_2 at $T = (675 \pm 3)$ K. It is stable in a rather narrow temperature interval and disproportionates to $Ni_{1-\delta}S$ and $Ni_{3\pm\delta}S_2$ at $T = (850 \pm 2)$ K. The phases are characterized structurally, and a revised phase diagram is presented. The heat capacity of a sample with composition Ni_7S_6 was determined over the temperature range $T = 5$ K to 970 K by adiabatic calorimetry. Effects from metastable modifications of the high-temperature phase were observed during thermal analysis, X-ray diffraction, and calorimetry on incompletely equilibrated samples. Thermodynamic-function values for Ni_7S_6 and Ni_9S_8 are presented.

1. Introduction

The nickel sulfides and the phase relations for (nickel + sulfur) have been subject to extensive studies. The sulfur-rich part of the system appears to be rather simple with Ni_3S_4,[1-3] and NiS_2,[2-4] as the only phases. A more nickel-rich part, covering $x \approx 0.40$ to 0.50 for $Ni_{1-x}S_x$, may for the present purpose be subdivided into three different composition regions. For two of these regions the phase relations are fairly well established. They concern the low- and high-temperature modifications of Ni_3S_2,[3,5,6] and of NiS.[3,7,8] For the intermediate-composition region, covering $x = 0.45$ to 0.48, the results are quite contradictory. Phases with composition Ni_6S_5,[2,9-11] Ni_7S_6,[2,10,12-16] and Ni_9S_8,[11,17,18] have been reported. Some investigators indicate the occurrence of two phases in this compositional region.

0021-9614/94/090987+14 $08.00/0

According to Lundqvist[2] and Sokolova,[11] a more nickel-rich low-temperature phase with composition Ni_7S_6,[2] or Ni_9S_8,[11] disproportionates into a high-temperature phase Ni_6S_5 and the more sulfur-rich $Ni_{1-\delta}S$ at around $T = 673$ K. In a more recent study, Kullerud and Yund[3] report, however, that the low-temperature and the high-temperature phases both have the composition Ni_7S_6. The high-temperature phase Ni_7S_6 decomposes into $Ni_{3\pm\delta}S_2$ and $Ni_{1-\delta}S$ at $T \approx 846$ K.[3]

This rather confusing situation was partly resolved through the single-crystal X-ray diffraction study by Fleet,[15] which confirmed that the high-temperature modification has the composition Ni_7S_6. More recently, Fleet[17,18] ascertained that the low-temperature modification has the composition Ni_9S_8 and is isostructural with the mineral godlevskite, described by Kulagov *et al.*[13] Whereas the crystal structure of Ni_9S_8 is well ordered,[17,18] a substantial fraction of the nickel atoms appear to be in approximately half-filled positions (about 24 of the 36 nickel positions in the unit cell) in the high-temperature phase Ni_7S_6.[15]

The electron-diffraction study by Putnis[16] added to the complexity in the $x = 0.45$ to 0.48 part of $\{(1-x)Ni+xS\}$ with the observation of several superstructures for rapidly cooled samples of Ni_7S_6. Thus, the phase relations in the $x = 0.45$ to 0.48 region need further exploration.

The present report concerns the stability fields of the $Ni_{7\pm\delta}S_6$ and Ni_9S_8 phases, as well as the structural properties of these phases, and the heat capacity of a sample with composition Ni_7S_6. The thermodynamic properties of Ni_7S_6 and Ni_9S_8 are evaluated. Related results have been reported for Ni_3S_2,[19] and will be presented for NiS,[20] whereas the conditions for the occurrence and the structural features of the various metastable phases with composition close to Ni_7S_6 are described in other papers.[21-23]

2. Experimental

Small-scale samples (mass: 0.5 to 1 g) were synthesized from weighed masses of the elements (turnings from nickel rod, 99.99 per cent, Johnson Matthey Laboratories, and sulfur lumps, 99.999 per cent, Koch–Light Laboratories) as starting materials. The samples were heated in closed evacuated silica-glass ampoules. After a first heating at $T = 823$ K, the samples were cooled to ambient temperature, crushed, and subjected to two or three annealing cycles until homogeneity was obtained. Some of the homogeneous samples were divided into smaller portions which, in turn, were subjected to heat treatment at different chosen annealing temperatures (in 50 K intervals between 373 K and 833 K).

A large-scale sample with nominal composition Ni_7S_6 (mass: ≈ 137 g) for the calorimetric measurements was prepared from the $Ni_{2.9}S_2$ sample used in an earlier study[19] and sulfur (small crystals, 99.9998 mass per cent pure from Koch-Light Laboratories). The mixture was heated at $T = 773$ K for 15 d and cooled to room temperature with the furnace.

All samples were characterized by room-temperature powder X-ray diffraction (p.x.d.) using Guinier–Hägg cameras (Cr $K\alpha_1$ or Cu $K\alpha_1$ radiation, Si as internal standard, $a = 543.1065$ pm.[24] $Ag_6Ge_{10}P_{12}$, with $a = 1031.25$ pm,[25] was used as

internal standard for samples with reflections at low scattering angles. High-temperature p.x.d. studies were conducted between $T = 300$ K and 1200 K using a Guinier–Simon camera (Enraf Nonius FR533) and chosen heating (and cooling) rates between 0.002 $K \cdot s^{-1}$ and 0.01 $K \cdot s^{-1}$. The samples were kept inside rotating evacuated and sealed silica-glass capillaries, and the temperature change was synchronized with the film movement. The temperature calibration was carried out by measurements of the known lattice-constant variation of silver with temperature.[26] The films were evaluated by means of a film comparator. Unit-cell dimensions were obtained by least-squares refinements using the CELLKANT program.[27] Simulation of powder diffractograms was done by means of the LAZY-PULVERIX program.[28]

Differential thermal analysis (d.t.a., d.s.c.) was carried out between $T = 300$ K and 1000 K using a Netzsch 404EP thermoanalyzer, and between $T = 300$ K and 900 K using a Mettler TA3000 system.

The cryogenic heat-capacity measurements at Ann Arbor were performed in the Mark X adiabatic cryostat.[29] A mass about 92 g of sample was loaded into the calorimeter with mass 39.593 g and internal volume 79.16 cm^3. In order to facilitate rapid thermal equilibration, a pressure 3.0 kPa at $T = 300$ K of He gas was introduced after prior evacuation of the calorimeter. The thermometer was calibrated by the U.S. National Bureau of Standards against IPTS-68, and was considered to reproduce thermodynamic temperatures within 0.03 K between 5 K and 300 K. The heat capacity of the empty calorimeter represented 10 per cent of the total heat capacity below $T = 50$ K, increasing to about 30 per cent at ambient temperature.

The high-temperature adiabatic-calorimetry apparatus and measuring technique at the University of Oslo have been described in detail earlier.[30,31] The computer-operated calorimeter was intermittently heated and surrounded by electronically controlled adiabatic shields. The sample with mass 110.86 g was enclosed in an evacuated vitreous-silica tube of about 50 cm^3 volume, tightly fitted into the silver calorimeter. A central entrant well in the tube served for the heater and Pt resistance thermometer. The resistance thermometer was calibrated locally at the ice, steam, Sn, Zn, and Sb points. The resistance was measured with an ASL-18 resistance bridge. The temperatures were judged to correspond to IPTS-68 to within 0.03 K up to 900 K and within 0.10 K above. The heat capacity of the empty calorimeter was determined in a separate series of experiments with a standard deviation of a single measurement from the smoothed heat-capacity curve of about 0.15 per cent. Corrections were applied for the differences in mass of the silica-glass containers. The accuracy of the heat-capacity determinaions was judged to be within 0.3 per cent, whereas the precision was around 0.2 per cent.

3. Results and discussion

STRUCTURAL PROPERTIES AND PHASE EXTENSION

$Ni_{7\pm\delta}S_6$: Equilibrium calorimetry, d.t.a., and high-temperature powder X-ray diffraction results, show that $Ni_{7\pm\delta}S_6$ forms eutectoidally from Ni_9S_8 and Ni_3S_2 at

TABLE 1. Miller indices, lattice spacing, and relative observed intensities for Ni_7S_6 at $T = 743$ K. Diffraction results collected with a Siemens D500 diffractometer (N_2-atmosphere) for a thin powder sample deposited on a platinum heating element. Cu $K\alpha_1$-radiation, $\lambda = 154.060$ pm

H	K	L	$\frac{d}{\text{pm}}$	$\frac{I_{obs}}{I_{max}}$	H	K	L	$\frac{d}{\text{pm}}$	$\frac{I_{obs}}{I_{max}}$
0	0	2	820.2	0.071	0	4	5	215.9	0.051
0	2	0	571.9	0.053	1	3	4	212.6	0.130
0	2	2	469.6	0.104	1	3	5	198.3	0.409
0	0	4	411.4	0.258	0	4	6	197.9	
0	2	3	395.9	0.021	0	2	8	193.6	0.127
0	2	4	334.0	0.057	0	6	1	189.4	0.071
1	1	0	314.7	0.038	1	1	7	188.3	0.490
1	1	2	293.9	0.202	1	5	1	186.3	0.324
0	4	0	285.9	0.056	1	3	6	184.1	0.128
0	2	5	285.2		1	5	2	182.8	0.227
0	4	1	281.7	0.135	0	4	7	181.6	0.176
1	1	3	272.9	1.000	1	5	3	177.4	0.380
0	0	6	274.3		0	2	9	174.2	0.067
0	4	2	270.1	0.051	0	6	4	173.0	0.126
0	2	6	247.3	0.303	1	1	8	172.2	0.193
1	3	0	248.4		1	3	7	170.7	0.167
1	3	1	245.6	0.439	1	5	4	170.6	
1	3	2	237.8	0.067	0	6	5	165.0	0.425
0	4	4	234.8	0.052	0	0	10	164.6	
0	2	7	217.4	0.026	2	0	0	163.7	0.078

$T = (675 \pm 3)$ K and that it decomposes to $Ni_{1-\delta}S$ and $Ni_{3\pm\delta}S_2$ at $T = (850 \pm 2)$ K. The decomposition products were confirmed by p.x.d. studies. The present findings regarding the thermal stability of $Ni_{7\pm\delta}S_6$ concur well with literature values.[3]

$Ni_{7\pm\delta}S_6$ is orthorhombic (space group (*Bmmb*) with $a = (327.4 \pm 0.1)$ pm, $b = (1615.7 \pm 0.7)$ pm, $c = (1135.9 \pm 0.4)$ pm, and $V_m/L = (31.13 \pm 0.04) \cdot 10^6$ pm^3 for $Ni_{1.1658}S$, where V_m denotes molar volume and L Avogadro's constant.[15] The single crystal studied by Fleet[15] showed additional weak superstructure reflections which were not accounted for in the structure refinement. In agreement with these observations, it proved impossible in the present study to retain the disordered orthorhombic structure of $Ni_{7\pm\delta}S_6$ on quenching. The $Ni_{7\pm\delta}S_6$ phase always transformed into metastable phases with closely related structures.[21-23] Actually, all available p.x.d. results for quenched specimens apparently refer to the metastable modifications and do not seem to correspond to the high-temperature phase designated here as $Ni_{7\pm\delta}S_6$. Furthermore, these superstructures explain why several Bragg reflections, non-indexable according to the above unit cell for $Ni_{7\pm\delta}S_6$, have been reported for samples in this composition range.

Information about the structural arrangement of the $Ni_{7\pm\delta}S_6$ phase can be obtained from high-temperature p.x.d. results. The observed diffraction pattern at $T = 743$ K agrees fairly well with that calculated from the structural results by Fleet[15] using the LAZY-PULVERIX program,[28] with respect both to intensities and to systematic absences. Observed intensities, lattice spacings, and Miller indices are given in table 1.

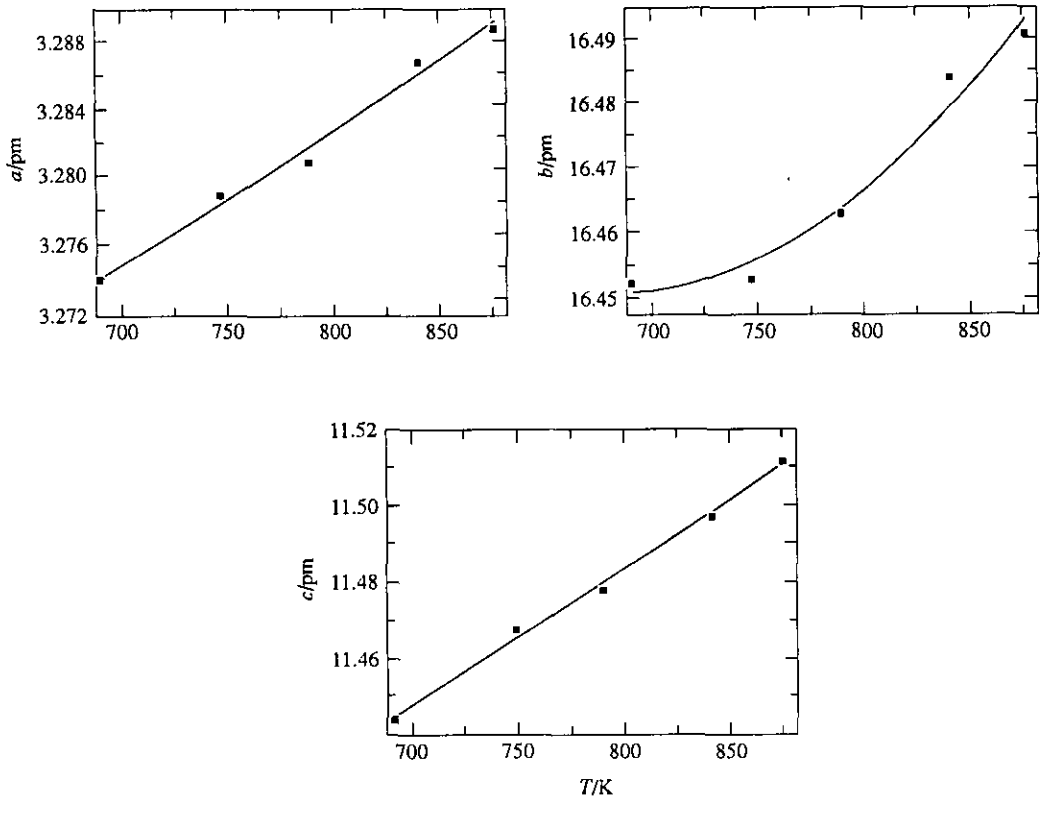

FIGURE 1. Lattice constants for Ni_7S_6 from $T = 675$ K to 875 K.

Thermal expansivities for stoichiometric Ni_7S_6 have been calculated on the basis of the temperature variation of the unit-cell dimensions shown in figure 1. Over the temperature range 693 K to 833 K the expansivity was approximated as linear with $\alpha = 7.4 \cdot 10^{-5}\ K^{-1}$.

Due to the superstructure formation, the width of the homogeneity region of the $Ni_{7\pm\delta}S_6$ phase could not be obtained from the variation of the unit-cell dimensions for the quenched samples. For this purpose, d.t.a. and high-temperature p.x.d. were used. Careful evaluation of high-temperature p.x.d. patterns, collected for specimens

TABLE 2. Unit-cell dimensions of the Ni_7S_6 phase at $T = 773$ K

x in Ni_xS	a/pm	b/pm	c/pm
1.140	328.83 ± 0.08	1652.2 ± 0.4	1150.1 ± 0.3
1.170	329.17 ± 0.08	1653.0 ± 0.5	1151.3 ± 0.3
1.229	329.69 ± 0.09	1653.6 ± 0.5	1153.9 ± 0.3

with different over-all compositions on the same film at $T = 773$ K, gave small but significant variations in the unit-cell dimensions, see table 2. It should be noted that the *b*- and *c*-axis are 2.3 per cent and 1.3 per cent larger than observed at room temperature by Fleet.[15]

An estimate of the change in nickel content related to the observed change in unit-cell volume may be obtained by comparison with the volume change as a function of composition for the highly non-stoichiometric $Ni_{3\pm\delta}S_2$ phase.[32] The increase in volume per nickel atom in the non-stoichiometric range of $Ni_{3\pm\delta}S_2$ is then $8.6 \cdot 10^6$ pm^3. Based on an experimental density value, Fleet's structure refinement indicates that the unit cell of $Ni_{7\pm\delta}S_6$ contains 19.3 sulfur atoms and 22.5 nickel atoms. Thus, the observed volume change for Ni_7S_6 indicates a homogeneity range with a mole-fraction increment $\Delta x = 0.0056$ (0.5Ni per unit cell). This estimate is somewhat larger than the homogeneity region reported by Kullerud and Yund,[3] $x = 0.4576$ to 0.4622, *i.e.* $\Delta x = 0.0046$. None of the p.x.d. patterns for $Ni_{7\pm\delta}S_6$ at $T = 773$ K showed the presence of any other phases. This was not to be expected, however, since the detection limit of the Guinier–Simon camera is rather large at high temperatures compared with that for p.x.d. at ambient temperature.

Ni_9S_8: According to Fleet,[18] Ni_9S_8 is isostructural to the mineral godlevskite, originally discovered in the Noril'sk and Talnakh sulfide deposits.[13] The structure of a mineral sample with composition $(Ni_{8.7}Fe_{0.3})S_8$ was determined by Fleet[17] as orthorhombic (space group *C*222) with $a = (933.59 \pm 0.07)$ pm, $b = (1121.85 \pm 0.10)$ pm, $c = (943.00 \pm 0.06)$ pm. Slightly different lattice constants were observed for synthetic Ni_9S_8,[18] with unit-cell volume $V_m/L = 30.86 \cdot 10^6$ pm^3 for $Ni_{1.125}S$. The presently observed p.x.d. pattern for Ni_9S_8 agrees fully with the pattern calculated on the basis of the single-crystal structural results.

The compositional extension of Ni_9S_8 was investigated on the basis of samples quenched from $T = 653$ K and 623 K. The refined unit-cell dimensions remained constant within one calculated standard deviation. The average unit-cell dimensions for eight samples quenched from $T = 623$ K with composition between $Ni_{1.091}S$ and $Ni_{1.165}S$ are $a = (932.5 \pm 0.1)$ pm, $b = (1123.9 \pm 0.1)$ pm, and $c = (941.0 \pm 0.1)$ pm. For quenched samples with composition slightly outside the ideal 9/8 ratio, p.x.d. showed no indications of the neighboring phases NiS or Ni_3S_2. Nevertheless, taking the detection limit for the p.x.d. technique into account {which in this case was found to be (2 to 3) mass per cent of Ni_3S_2}, it is concluded that the Ni_9S_8 phase must exhibit a very narrow homogeneity range.

According to Kullerud and Yund,[3] the low-temperature modification of "Ni_7S_6" decomposes at $T = 675$ K and 672 K in equilibrium with NiS and Ni_3S_2, respectively. Present d.t.a. and high-temperature p.x.d. results, however, show that the Ni_9S_8 phase spans a wider temperature range than earlier assumed.[3] Visual inspection of the continuous high-temperature p.x.d. Guinier–Simon photographs (*e.g.* for the composition $Ni_{1.12}S$), clearly show that the phase transition between the high- and low-temperature modifications of NiS occurs at $\Delta T \approx 50$ K below the disproportionation of Ni_9S_8 into $Ni_{1-\delta}S$ and $Ni_{7\pm\delta}S_6$. Endothermal effects were observed in d.t.a. recordings of samples with composition $Ni_{1.11}S$ and $Ni_{1.16}S$. In the former, the endothermal effects occur at $T = (652 \pm 5)$ K and at (709 ± 5) K. The $T = (652 \pm 5)$ K effect is attributed to the NiS transition,[3,20] and the latter to the

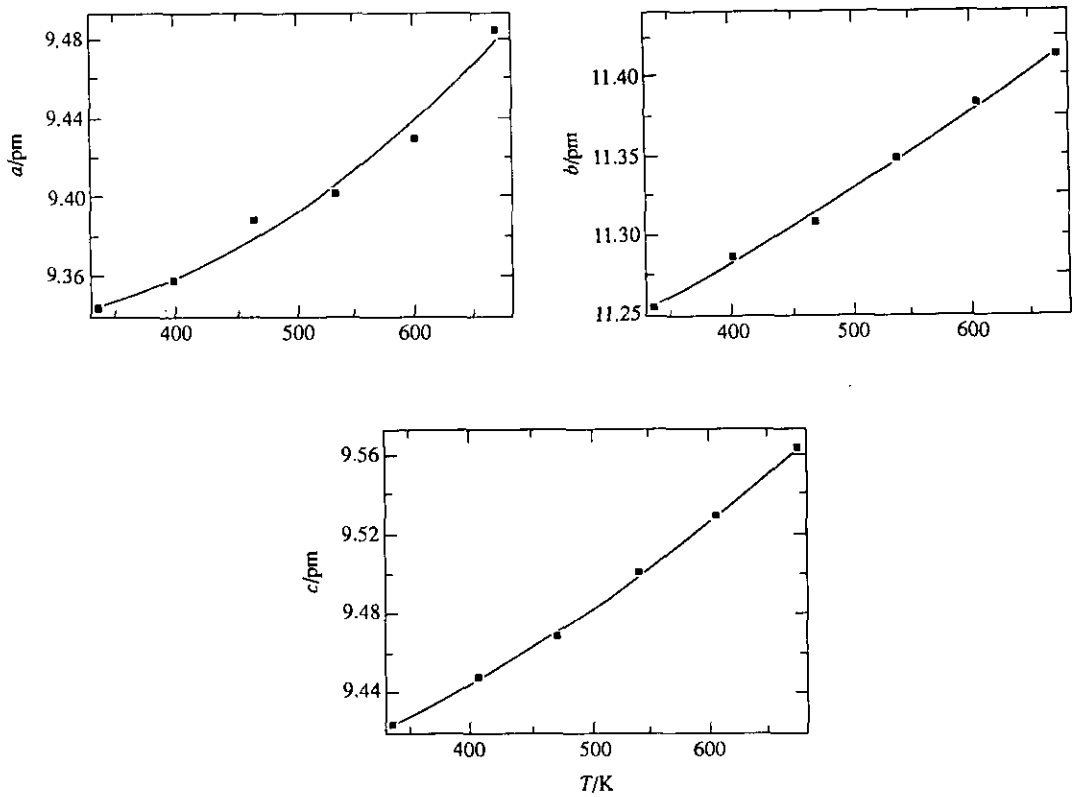

FIGURE 2. *Lattice constants for* Ni_9S_8 *from* $T = 340$ K *to* 690 K.

disproportionation of the Ni_9S_8 phase, which is stable at all temperatures below 709 K. In $Ni_{1.16}S$, effects are observed at $T = (675 \pm 3)$ K and at (709 ± 5) K. The $T = (673 \pm 3)$ K effect on heating signalizes the formation of $Ni_{7\pm\delta}S_6$.

Ni_9S_8 shows normal thermal expansion over its entire stability interval, see figure 2. The thermal expansivity was approximated as linear with $\alpha = 12 \cdot 10^{-5}\ K^{-1}$.

HEAT CAPACITY

The experimental heat capacities for a sample with overall composition Ni_7S_6 are given in chronological order in table 3 and are presented graphically in figure 3. The approximate temperature increments in the measurements can usually be inferred from the adjacent mean temperatures in table 3. The estimated standard deviation of a single heat-capacity measurement is about $0.003 \cdot C_{p,m}$. In table 4 the heat capacity in the transitonal region is given together with enthalpy and entropy increments. The Detn. A results are somewhat lower than those of Detn. B.† The latter results are considered to be more accurate because of more complete equilibration, whereby the structurally disordered $Ni_{7\pm\delta}S_6$ phase is also removed.

† Note added in proof. An even lower value: $\Delta_{trs}H^{\circ}_{m}\{(1/13)Ni_7S_6\}/R = (90.2 \pm 5.4)$ K, was reported in the d.s.c. work by M. Dubusc *et al.* in *C.R. Acad. Sci. Paris C* **1980**, 290, 89.

TABLE 3. Experimental values for the heat capacity of $(1/13)Ni_7S_6$ ($R = 8.3145\ J \cdot K^{-1} \cdot mol^{-1}$; $M\{(1/13)Ni_7S_6\} = 46.402\ g \cdot mol^{-1}$)

T/K	$C_{p,m}/R$	T/K	$C_{p,m}/R$	T/K	$C_{p,m}/R$	T/K	$C_{p,m}/R$	T/K	$C_{p,m}/R$	T/K	$C_{p,m}/R$
High-temperature results—University of Oslo											
Series I		547.39	3.265	679.24	3.979	811.39	4.449	440.18	3.197	416.72	3.156
314.01	2.874	557.77	3.329	684.88	4.005	820.36	4.603	448.21	3.206	426.68	3.169
321.78	2.937	568.04	3.387	690.50	4.051	ΔH	detn. C	456.19	3.220	436.64	3.178
330.84	2.968	578.29	3.417	696.13	4.082	861.27	4.344	464.10	3.228	446.63	3.193
341.20	2.986	588.50	3.442	701.72	4.113	874.66	4.382	493.96	3.255	456.64	3.198
351.56	3.013	598.68	3.476	707.28	4.171	887.03	4.373	504.03	3.280	466.66	3.211
361.81	3.037	608.82	3.507	712.82	4.197	900.64	4.437	514.10	3.303	476.70	3.226
371.97	3.054	618.91	3.531	718.37	4.268	914.17	4.492	524.15	3.387	486.78	3.243
382.10	3.072	629.11	3.580	723.94	4.331	927.70	4.537	534.03	3.590	496.87	3.249
392.23	3.061	639.66	3.636	729.51	4.412	941.21	4.593	544.00	3.400	516.25	3.271
402.56	2.927	650.30	3.689	735.06	4.424	954.69	4.669	554.19	3.381	526.40	3.301
413.27	2.652	ΔH	detn. A	740.77	4.222	968.14	4.719	564.43	3.415	546.74	3.327
424.14	2.682	Series II		746.58	4.212	Series IV		Series V		556.94	3.369
434.82	2.837	650.50	3.706	752.32	4.216	335.98	2.967	306.87	2.891	567.16	3.376
445.24	3.089	654.23	3.725	757.99	4.216	347.28	3.008	317.06	2.929	577.41	3.410
455.43	3.232	657.94	3.756	763.68	4.223	364.81	3.050	337.25	2.989	587.71	3.430
465.67	3.232	661.62	3.829	774.77	4.250	374.71	3.086	347.26	3.010	598.04	3.454
475.87	3.267	665.26	3.940	780.20	4.267	384.66	3.087	357.21	3.034	Series VI	
485.91	3.289	668.79	4.027	785.92	4.261	394.56	3.120	367.12	3.063	267.91	2.814
496.07	3.264	ΔH	detn. B	791.79	4.487	404.51	3.129	377.03	3.081	273.66	2.810
506.38	3.203	Series III		796.93	4.511	414.30	3.150	386.93	3.103	279.34	2.785
516.83	3.109	661.86	3.887	801.67	4.623	423.62	3.164	396.86	3.120	286.64	2.846
527.13	3.506	667.68	3.918	806.45	4.638	432.10	3.180	406.79	3.138	295.60	2.877
537.16	3.552	673.46	3.949							304.53	2.894
Low-temperature results—University of Michigan											
Series VII		116.876	1.714	179.620	2.310	251.415	2.709	14.440	0.0224	39.250	0.325
59.417	0.703	121.843	1.784	184.995	2.329	256.466	2.774	16.091	0.0303	41.649	0.364
66.994	0.856	126.862	1.859	190.358	2.385	261.564	2.775	17.528	0.0390	44.044	0.410
70.308	0.917	131.921	1.909	200.747	2.442	266.661	2.791	18.997	0.049	46.505	0.461
77.207	1.053	137.039	1.952	205.904	2.474	Series VIII[a]		20.512	0.065	49.163	0.505
80.906	1.118	142.328	2.000	210.854	2.523	5.636	0.0014	22.165	0.078	52.052	0.550
84.748	1.197	147.599	2.059	215.855	2.530	6.652	0.0022	23.550	0.091	55.001	0.613
88.802	1.165	152.774	2.108	220.966	2.558	7.410	0.0031	25.610	0.116	57.915	0.674
93.137	1.340	158.090	2.178	226.107	2.593	8.527	0.0048	29.007	0.158		
97.547	1.405	163.382	2.201	236.221	2.641	9.602	0.0067	30.717	0.181		
107.061	1.566	168.936	2.233	241.392	2.670	11.765	0.0129	32.761	0.221		
111.954	1.637	174.217	2.272	246.356	2.687	12.913	0.0162	34.878	0.251		

[a] After measurements to $T = 350$ K.

The equilibrated Ni_7S_6 sample is a two-phase mixture below $T \approx 675$ K, consisting of Ni_3S_2 and Ni_9S_8. The $Ni_{7\pm\delta}S_6$ phase has a substantial homogeneity region which appears to include the 7/6 composition up to $T \approx 730$ K. The thermal effect at this temperature is probably due to the separation of $Ni_{1-\delta}S$ from single phase $Ni_{7\pm\delta}S_6$. At $T \approx 850$ K, $Ni_{7\pm\delta}S_6$ disproportionates into $Ni_{3\pm\delta}S_2$ and $Ni_{1-\delta}S$.

The Series I results were obtained directly after the synthesis (annealing at $T = 773$ K for 15 d; cooling to room temperature with the furnace). Two smaller

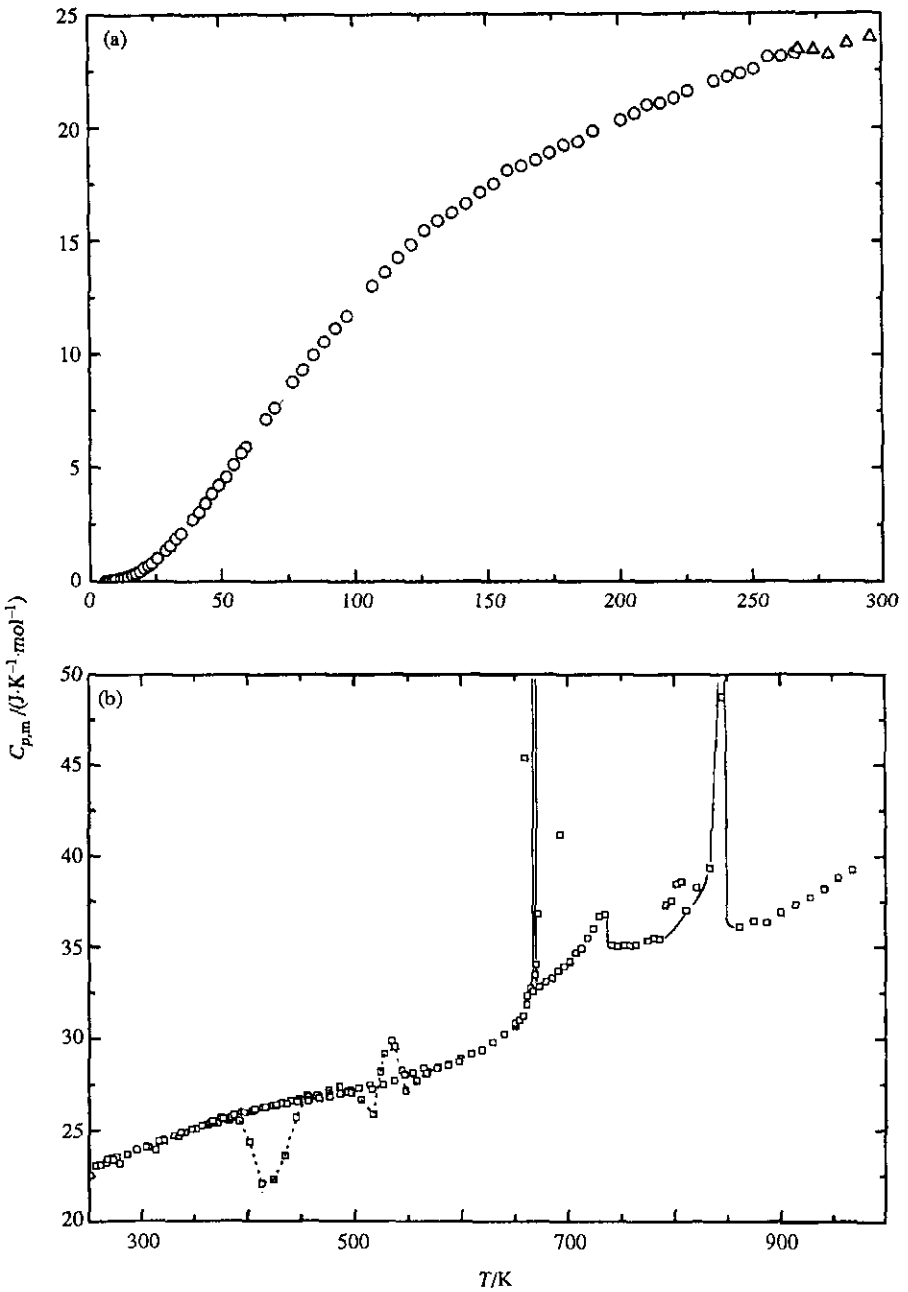

FIGURE 3. Molar heat capacity of (1/13)Ni_7S_6 (over-all composition) (a), from $T = 5$ K to 300 K; (b), from $T = 250$ K to 1000 K.

TABLE 4. Fractional molar enthalpies of transition for (1/13)Ni_7S_6 ($R = 8.3145\ J \cdot K^{-1} \cdot mol^{-1}$)

$\langle T \rangle$/K	ΔT/K	$C_{p,m}/R$	$C_{p,m}(n.t.)/R$	$\Delta_{trs}H_m/R \cdot K$	T_{fin}/K	$\Delta_{trs}S_m/R$
		$M\{(1/13)Ni_7S_6\} = 46.402\ g \cdot mol^{-1}$				
Detn. A						
Series I, Detn. 35 to 39						
659.97	8.88621	6.044	3.774	20.178	664.40921	0.03057
669.78	10.7467	4.093	3.847	2.636	675.15594	0.00393
677.26	4.20449	18.859	3.909	62.856	679.36043	0.09281
683.70	8.67048	6.054	3.964	18.124	688.03091	0.02651
692.94	9.82108	4.950	4.045	8.894	697.35199	0.01283
				112.68		0.16665
Detn. B						
Series II, Detn. 7 to 12						
672.19	3.34913	4.428	3.864	1.889	673.86481	0.00281
674.56	1.39377	40.856	3.885	51.529	675.25858	0.07638
675.27	0.03060	1031.8	3.890	31.455	675.28918	0.04658
675.81	1.03894	25.329	3.894	22.270	676.32812	0.03295
677.23	1.80416	12.220	3.910	14.992	678.13228	0.02214
679.35	2.43643	7.643	3.923	9.064	680.56871	0.01334
				131.20		0.19420
Detn. C						
Series III, Detn. 30 to 33						
832.78	12.6958	4.629	4.297	4.215	839.12557	0.00506
844.79	11.3284	5.757	4.314	16.347	850.45393	0.01935
850.50	0.09714	1354.98	4.322	131.20	850.55107	0.15426
852.58	4.05824	59.102	4.326	222.29	854.60931	0.26073
				374.05		0.43940

heat-capacity effects were observed at $T \approx 415$ K and 515 K, see figure 4. Slight but yet significant temperature-drift rates were connected with these anomalies. The first transition (at $T \approx 415$ K) gave rise to positive drift rates, indicating an exothermal transformation, whereas the latter (at $T \approx 515$ K) apparently consisted of an exothermal enthalpy effect superimposed on a larger endothermal effect (with maximum at $T \approx 535$ K). Series II refers to measurements performed after exploratory runs in the region between $T \approx 670$ K and 720 K for 40 d, whereas Series III pertains to measurements after annealing the sample at $T \approx 810$ K for 2 d.

The two low-temperature anomalies disappeared after annealing at $T = 485$ K (12 d) and 560 K (5 d), respectively, see Series IV and V in table 3 and figure 4. This indicates that the effects are due to reactions involving metastable phases which are formed on cooling Ni_7S_6 in the sample preparation step.[21]

The endothermal heat-capacity anomaly at $T \approx 535$ K was also observed in an earlier study of $Ni_{2.9}S_2$ (a two-phase mixture of Ni_3S_2 and Ni_9S_8).[19] The effect was at that time, in the absence of knowledge about the metastable phases, suggested as originating from traces of NiO, Ni_3S_4, or cristobalite, see table 1 in reference 19.

These small thermal effects are of minor importance in the derivation of the thermodynamic properties of Ni_9S_8 and $Ni_{7\pm\delta}S_6$. In the evaluation of the

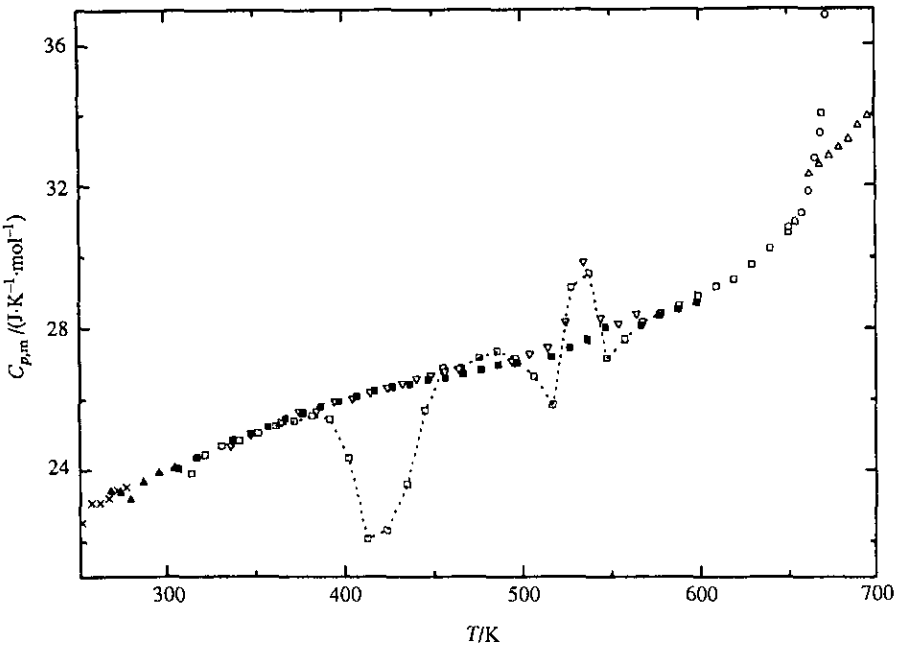

FIGURE 4. Molar heat capacity of (1/13)Ni_7S_6 (over-all composition) from $T = 250$ K to 700 K. □, Series I; ○, series II; △, series III; ▽, series IV; ■, series V; ▲, series VI; ×, series VII.

thermodynamic properties, only those results were used which were not influenced by these effects.

THERMODYNAMIC PROPERTIES

The experimental heat capacities for the low- and high-temperature regions were fitted to polynomials in temperature by the least-squares method. The two sets of measurements (UofM and UofO) were joined across the temperature region from $T = 210$ K to 260 K, due to a slight mismatch between the results in this region. The enthalpy and entropy of the two-phase sample with overall composition Ni_7S_6 were evaluated by integrating the heat-capacity polynomials in temperature and by adding transitional enthalpies and entropies, see table 5. The thermodynamic-function values at the lowest temperatures were obtained by extrapolation of the approximately linear relation between $C_V \cdot T^{-1}$ and T^2. The resulting value of the electronic heat-capacity coefficient γ was zero within experimental accuracy. The value is, however, burdened by a rather large uncertainty as the estimate is based on results in the temperature range from $T = 5.6$ K and 16.1 K, only. In order to obtain a more correct value of γ, heat-capacity results at even lower temperatures are needed.

The molar heat capacities and thermodynamic functions for Ni_9S_8 were obtained from the thermodynamic properties for the sample with composition Ni_7S_6 by adjusting for the presence of Ni_3S_2 in the sample.

TABLE 5. Molar thermodynamic properties of (1/13)Ni_7S_6 and of (1/17)Ni_9S_8. The former is a two-phase mixture of Ni_9S_8 and Ni_3S_2 up to $T = 675.3$ K, and consists of two phases ($Ni_{3\pm\delta}S_2$ and $Ni_{1-\delta}S$) also above $T = 850.5$ K ($R = 8.3145\ J \cdot K^{-1} \cdot mol^{-1}$)

$\frac{T}{K}$	$\frac{C_{p,m}}{R}$	$\frac{\Delta_0^T S_m^\circ}{R}$	$\frac{\Delta_0^T H_m^\circ}{R \cdot K}$	$\frac{\Phi_m^\circ}{R}$	$\frac{T}{K}$	$\frac{C_{p,m}}{R}$	$\frac{\Delta_0^T S_m^\circ}{R}$	$\frac{\Delta_0^T H_m^\circ}{R \cdot K}$	$\frac{\Phi_m^\circ}{R}$
				$M\{(1/13)Ni_7S_6\} = 46.402\ g \cdot mol^{-1}$					
5	0.001	0	0.001	0	340	2.994	3.711	648.84	1.802
10	0.008	0.003	0.019	0.001	360	3.039	3.883	709.18	1.913
15	0.025	0.009	0.096	0.003	380	3.081	4.049	770.39	2.021
20	0.058	0.020	0.295	0.005	400	3.119	4.208	832.40	2.127
25	0.107	0.038	0.699	0.010	420	3.154	4.361	895.13	2.229
30	0.172	0.063	1.391	0.017	440	3.186	4.508	958.53	2.330
35	0.250	0.095	2.443	0.025	460	3.215	4.650	1022.5	2.427
40	0.337	0.134	3.907	0.036	480	3.244	4.788	1087.1	2.523
45	0.427	0.179	5.818	0.050	500	3.272	4.921	1152.3	2.616
50	0.521	0.229	8.186	0.065	520	3.301	5.050	1218.0	2.707
60	0.715	0.341	14.357	0.102	540	3.334	5.175	1284.4	2.796
70	0.911	0.466	22.489	0.145	560	3.371	5.297	1351.4	2.884
80	1.103	0.600	32.569	0.193	580	3.417	5.416	1419.3	2.969
90	1.286	0.740	44.525	0.245	600	3.474	5.533	1488.2	3.052
100	1.455	0.885	58.24	0.303	620	3.545	5.648	1558.3	3.134
110	1.610	1.031	73.58	0.362	640	3.635	5.762	1630.1	3.215
120	1.749	1.177	90.38	0.424	660	3.846	5.876	1704.7	3.293
130	1.873	1.322	108.51	0.487	675.3	1031.8	6.089	1848.0	3.352
140	1.983	1.465	127.80	0.552	680	3.977	6.184	1913.0	3.371
150	2.080	1.605	148.12	0.618	700	4.111	6.301	1993.8	3.453
160	2.166	1.742	169.36	0.684	720	4.286	6.419	2077.7	3.533
170	2.244	1.876	191.42	0.750	735	4.441	6.509	2143.1	3.593
180	2.314	2.006	214.21	0.816	735	4.203	6.509	2143.1	3.593
190	2.378	2.133	237.68	0.882	740	4.213	6.538	2164.1	3.613
200	2.439	2.257	261.77	0.948	760	4.221	6.650	2248.5	3.691
210	2.499	2.377	286.45	1.013	780	4.253	6.760	2333.1	3.769
220	2.559	2.494	311.75	1.076	800	4.600	6.874	2423.3	3.845
230	2.615	2.609	337.63	1.141	820	4.570	6.984	2512.5	3.920
240	2.665	2.722	364.04	1.205	850.5	1355.0	7.323	2798.1	4.033
250	2.711	2.832	390.94	1.268	860	4.341	7.632	3061.7	4.071
260	2.752	2.939	418.25	1.330	880	4.380	7.732	3148.9	4.154
270	2.789	3.043	445.96	1.392	900	4.435	7.831	3237.0	4.234
280	2.824	3.146	474.03	1.453	920	4.505	7.930	3326.4	4.314
290	2.856	3.245	502.43	1.513	940	4.589	8.027	3417.3	4.392
300	2.887	3.343	531.15	1.572	960	4.685	8.125	3510.0	4.469
320	2.943	3.531	589.46	1.689	970	4.738	8.173	3557.1	4.506
				$M\{(1/17)Ni_9S_8\} = 46.16106\ g \cdot mol^{-1}$					
5	0.002	0.000	0.002	0.000	220	2.562	2.550	315.06	1.116
10	0.010	0.004	0.024	0.002	230	2.622	2.666	340.98	1.183
15	0.030	0.011	0.118	0.004	240	2.675	2.779	367.48	1.247
20	0.068	0.024	0.355	0.006	250	2.723	2.889	394.74	1.310
25	0.124	0.046	0.826	0.013	260	2.766	2.997	421.94	1.373
30	0.195	0.074	1.619	0.020	270	2.804	3.102	449.78	1.436
35	0.278	0.110	2.801	0.030	280	2.840	3.206	478.00	1.498
40	0.370	0.153	4.419	0.042	290	2.874	3.304	506.57	1.559
45	0.463	0.202	6.503	0.058	300	2.906	3.404	535.48	1.618
50	0.557	0.256	9.050	0.075	320	2.961	3.592	594.15	1.736
60	0.751	0.374	15.577	0.115	340	3.007	3.773	653.81	1.850
70	0.944	0.505	24.055	0.161	360	3.051	3.946	714.37	1.962

TABLE 5—*continued*

$\frac{T}{K}$	$\frac{C_{p,m}}{R}$	$\frac{\Delta_0^T S_m^\circ}{R}$	$\frac{\Delta_0^T H_m^\circ}{R\cdot K}$	$\frac{\Phi_m^\circ}{R}$	$\frac{T}{K}$	$\frac{C_{p,m}}{R}$	$\frac{\Delta_0^T S_m^\circ}{R}$	$\frac{\Delta_0^T H_m^\circ}{R\cdot K}$	$\frac{\Phi_m^\circ}{R}$
80	1.133	0.643	34.453	0.213	380	3.091	4.113	775.84	2.071
90	1.314	0.786	46.701	0.266	400	3.127	4.272	838.00	2.178
100	1.481	0.934	60.685	0.327	420	3.160	4.425	900.90	2.280
110	1.634	1.083	76.280	0.389	440	3.191	4.573	964.40	2.382
120	1.771	1.230	93.305	0.453	460	3.218	4.715	1028.5	2.479
130	1.890	1.377	111.64	0.518	480	3.245	4.853	1093.1	2.576
140	1.996	1.521	131.08	0.584	500	3.273	4.986	1158.3	2.669
150	2.088	1.662	151.50	0.653	520	3.302	5.116	1224.0	2.761
160	2.170	1.799	172.80	0.720	540	3.338	5.241	1290.5	2.850
170	2.244	1.934	194.87	0.787	560	3.380	5.363	1357.6	2.938
180	2.311	2.063	217.64	0.854	580	3.437	5.482	1425.8	3.024
190	2.373	2.190	241.07	0.921	600	3.508	5.600	1495.2	3.107
200	2.434	2.314	265.12	0.988	620	3.601	5.717	1566.2	3.189
210	2.497	2.434	289.75	1.054	640	3.722	5.833	1639.4	3.272

PHASE RELATIONS

On the basis of the present investigation and results of our previous calorimetric studies on NiS,[20] Ni_3S_2,[19] and $Ni_{2.9}S_2$,[19] a revised version of the phase diagram for the mole-fraction range $x = 0.44$ to 0.48 is presented, see figure 5. The stability fields of the two intermediate phases—the highly ordered and stoichiometric Ni_9S_8

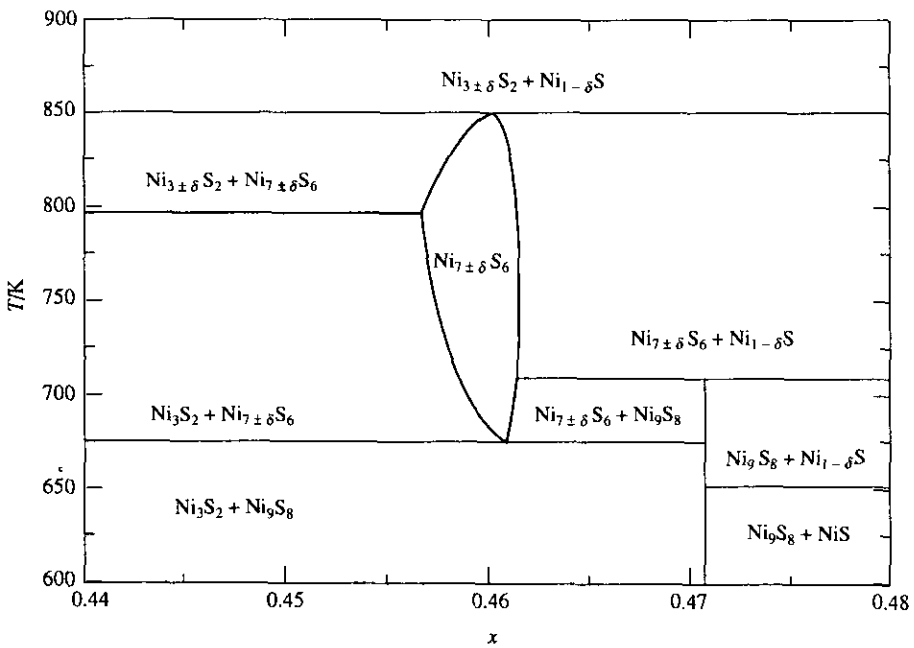

FIGURE 5. Phase diagram for the $\{(1-x)Ni+xS\}$ condensed system for $x = 0.44$ to 0.48.

and the disordered and non-stoichiometric $Ni_{7\pm\delta}S_6$—differ from earlier estimates. Ni_9S_8 is found here to disproportionate at $T = (709 \pm 2)$ K to $Ni_{1-\delta}S$ and $Ni_{7\pm\delta}S_6$. The non-stoichiometric $Ni_{7\pm\delta}S_6$-phase is stable from T = 675 K to 850 K, while the extension of its composition region is influenced considerably by phase transformations which take place in the neighboring Ni_9S_8 and Ni_3S_2 phases. Hence, the formation of the highly non-stoichiometric $Ni_{3\pm\delta}S_2$ phase at $T = 797$ K is expected considerably to diminish the stability field of $Ni_{7\pm\delta}S_6$ on the nickel-rich side. The formation of $Ni_{1-\delta}S$ at $T = 709$ K has somewhat less influence on the extension of the $Ni_{7\pm\delta}S_6$ phase on the sulfur-rich side. Thus, a maximum compositional extension of the phase is expected in the intermediate-temperature region, that is between $T = 709$ K and 797 K.

A homogeneity range from $x \approx 0.4622$ to 0.4576 at $T = 773$ K,[11] is in agreement with the present estimate. The small maximum in heat capacity at $T = 730$ K for the sample studied here presumably indicates the sulfur-rich composition limit of single phase $Ni_{7\pm\delta}S_6$.

The authors wish to thank Norges forskningsråd for financial support.

REFERENCES

1. Menzer, G. *Z. Krist.* **1926,** 64, 506.
2. Lundqvist, D. *Arkiv Kemi Mineral. Geol.* **1947,** 24A, No. 12.
3. Kullerud, G.; Yund, R. A. *J. Petrol.* **1962,** 3, 126.
4. Jong, W. F. de; Willems, H. W. *Z. anorg. Chem.* **1927,** 160, 185.
5. Rau, H. *J. Phys. Chem. Solids* **1976,** 37, 929.
6. Lin, R. Y.; Hu, D. C.; Chang, Y. A. *Metal. Trans.* **1978,** 9B, 531.
7. Rau, H. *J. Phys. Chem. Solids* **1975,** 36, 1199.
8. Black, S. N.; Jefferson, D. A.; Henderson, P. *J. Solid State Chem.* **1984,** 53, 76.
9. Schenck, R.; Forst, P. von der *Z. anorg. allgem. Chem.* **1939,** 241, 145.
10. Rosenqvist, T. *J. Iron Steel Inst.* **1954,** 176, 37.
11. Sokolova, M. A. *Doklady Akad. Nauk. SSSR* **1956,** 106, 286.
12. Peyronell, G.; Pacilli, E. *Atti R Accad. Ital* **1942,** 3, 278.
13. Kulagov, E. A.; Evstigneeva, T. L.; Yushko-Zakharova, O. E. *Geol. Rudnykh. Mestorozhdenii* **1969,** 11, 115.
14. Naldrett, A. J.; Gasparrini, E.; Buchan, R.; Muir, J. E. *Can. Mineral.* **1972,** 11, 879.
15. Fleet, M. E. *Acta Cryst.* **1972,** B28, 1237.
16. Putnis, A. *Am. Mineral.* **1976,** 61, 322.
17. Fleet, M. E. *Acta Cryst.* **1987,** C43, 2255.
18. Fleet, M. E. *Can. Mineral.* **1988,** 26, 283.
19. Stølen, S.; Grønvold, F.; Westrum, E. F., Jr.; Kolonin, G. R. *J. Chem. Thermodynamics* **1991,** 23, 77.
20. Grønvold, F.; Stølen, S. unpublished results.
21. Seim, H.; Fjellvåg, H.; Grønvold, F.; Stølen, S. unpublished results.
22. Hansen, V.; Seim, H.; Fjellvåg, H.; Olsen, A. *Micron and Microscopia Acta* **1992,** 23, 177.
23. Hansen, V.; Seim, H.; Fjellvåg, H.; Olsen, A. to be published.
24. Deslatters, R. D.; Henins, A. *Phys. Rev. Lett.* **1973,** 31, 972.
25. Fjellvåg, H.; Hönhle, W. unpublished results.
26. Spreadborough, J.; Christian, J. W. *J. Sci. Instrum.* **1959,** 36, 116.
27. Ersson, N. O. *CELLKANT program.* Chem. Inst. Univ. of Uppsala: Sweden. **1981.**
28. Parthé, E.; Yvon, K.; Jeitschko, W. *J. Appl. Cryst.* **1977,** 10, 73.
29. Westrum, E. F., Jr.; Furukawa, G. T.; McCullough, J. P. *Experimental Thermodynamics, Vol. I.* McCullough, J. P.; Scott, D. W.: Editors. Butterworths: London: 1968, p. 113.
30. Grønvold, F. *Acta Chem. Scand.* **1967,** 21, 1695.
31. Grønvold, F. *J. Chem. Thermodynamics* **1993,** 25, 1133.
32. Fjellvåg, H.; Andersen, A. *Acta Chem. Scand.* **1994,** 48, 290.